PCCP

PAPER

Cite this: *Phys. Chem. Chem. Phys.*, 2017, **19**, 3955

Mechanism of activated chemiluminescence of cyclic peroxides: 1,2-dioxetanes and 1,2-dioxetanones†

Felipe A. Augusto,[ab] Antonio Francés-Monerris,[bc] Ignacio Fdez. Galván,[b] Daniel Roca-Sanjuán,[c] Erick L. Bastos,[a] Wilhelm J. Baader*[a] and Roland Lindh*[b]

Received 29th November 2016,
Accepted 24th December 2016

DOI: 10.1039/c6cp08154a

www.rsc.org/pccp

Almost all chemiluminescent and bioluminescent reactions involve cyclic peroxides. The structure of the peroxide and reaction conditions determine the quantum efficiency of light emission. Oxidizable fluorophores, the so-called activators, react with 1,2-dioxetanones promoting the former to their first singlet excited state. This transformation is inefficient and does not occur with 1,2-dioxetanes; however, they have been used as models for the efficient firefly bioluminescence. In this work, we use the SA-CASSCF/CASPT2 method to investigate the activated chemiexcitation of the parent 1,2-dioxetane and 1,2-dioxetanone. Our findings suggest that ground state decomposition of the peroxide competes efficiently with the chemiexcitation pathway, in agreement with the available experimental data. The formation of non-emissive triplet excited species is proposed to explain the low emission efficiency of the activated decomposition of 1,2-dioxetanone. Chemiexcitation is rationalized considering a peroxide/activator supermolecule undergoing an electron-transfer reaction followed by internal conversion.

1 Introduction

The energy necessary to promote a chemical species to an electronically excited state can be obtained from a chemical reaction involving a high-energy intermediate (HEI).[1] This chemiexcitation is the key step of both chemi- and bioluminescent reactions, and four-membered cyclic peroxides such as 1,2-dioxetanes and 1,2-dioxenanones are the most common HEIs (Scheme 1).[2] The labile nature of such peroxides makes the isolation of the HEIs of important (bio)chemical processes, such as the firefly bioluminescence, extremely difficult or even impossible. However, the synthesis and isolation of several 1,2-dioxetanes and 1,2-dioxetanones allowed the study of chemi- and bioluminescence mechanisms and the development of several analytical methods.[3,4]

Thermal decomposition of 1,2-dioxetanes and 1,2-dioxetanones produces non-emissive triplet-excited carbonyl compounds.[5–7]

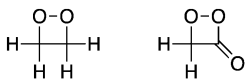

(**1**) (**2**)

Scheme 1 Parent 1,2-dioxetane (**1**) and 1,2-dioxetanone (**2**).

Energy transfer from the triplet carbonyl to an adequate fluorescent dye such as 9,10-dibromoanthracene results in visible sensitized light emission.[8] Interestingly, oxidizable fluorescent dyes can activate the decomposition of 1,2-dioxetanones, but not of 1,2-dioxetanes.[2] A chemical redox reaction between the 1,2-dioxetanone and the dye, named activator (ACT), produces ground state carbonyl compounds and leads to the excitation of the ACT to its first singlet excited state. The more oxidizable the ACT, the higher the light emission intensity and rate constant for peroxide decomposition, suggesting the occurrence of an electron-transfer step. Schuster and coauthors rationalized these results in terms of the Chemically Initiated Electron Exchange Luminescence (CIEEL) mechanism (Scheme 2).[9,10]

The CIEEL mechanism has been used not only to explain the activated chemiluminescence of 1,2-dioxetanones but also the emission of light in several other processes, including the firefly luciferin–luciferase bioluminescence,[11] the activated chemiluminescence of 1,2-dioxetanedione produced *in situ* (the so-called peroxyoxalate system),[1,12,13] the triggered decomposition of 1,2-dioxetanes bearing electron-rich substituents,[14,15] and the

[a] *Departamento de Química Fundamental, Instituto de Química, Universidade de São Paulo, Av. Prof. Lineu Prestes, 748, 05508-000, São Paulo, Brazil. E-mail: wjbaader@iq.usp.br*

[b] *Department of Chemistry—Ångström, Uppsala Center for Computational Chemistry, UC$_3$, Uppsala University, P.O. Box 518, SE-75120, Uppsala, Sweden. E-mail: roland.lindh@kemi.uu.se*

[c] *Instituto de Ciencia Molecular, Universitat de València, P.O. Box 22085, 46071, València, Spain*

† Electronic supplementary information (ESI) available: Cartesian coordinates of geometries from Table 1 and Fig. 3; details of the active space used in Table 2; nature of some molecular orbitals from Fig. 3. See DOI: 10.1039/c6cp08154a

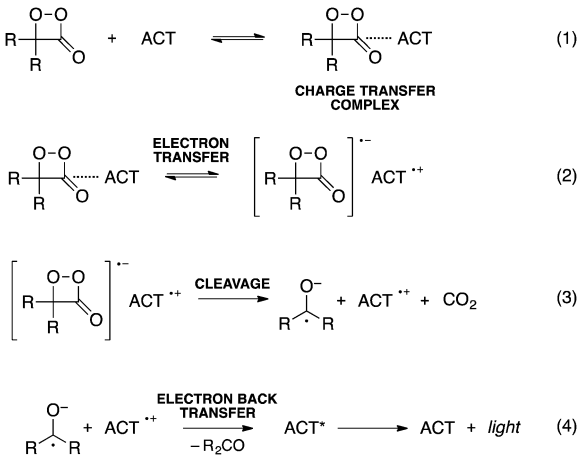

Scheme 2 The CIEEL mechanism. Step 1: formation of a charge transfer complex between a 1,2-dioxetanone and an ACT. Step 2: electron transfer from the ACT to the peroxide. Step 3: irreversible O–O and C–C bond breaking and formation of a radical ion pair between $R_2CO^{\bullet -}$ and $ACT^{\bullet +}$. Step 4: electron back transfer and chemiexcitation of the ACT followed by radiative relaxation of the ACT to the ground state.

chemiluminescence of diphenoyl peroxide.[10] However, the quantum efficiency of these processes varies from 0.1 to 100%[16,17] and, therefore, the occurrence of the CIEEL mechanism, and even its validity, has been questioned.[18,19] Alternative mechanisms for the chemical generation of electronic excited states have been proposed, with the most notorious example being the Charge-Transfer Induced Luminescence (CTIL) mechanism.[20–22] Although very similar, the CIEEL and CTIL mechanisms are grounded in complementary concepts that have been extensively used to explain chemical reactivity: electron transfer and charge transfer.[23] The intramolecular single electron transfer proposed by the CIEEL mechanism has been observed experimentally in the activated decomposition of appropriately substituted 1,2-dioxetanes;[24] whereas a charge transfer between an electron donor and the peroxide acceptor has been proposed in theoretical studies.[25,26] Both mechanisms propose the formation of a charge-transfer complex as the initial step.

This work examines the interaction of 1,2-dioxetanes and 1,2-dioxetanones with model activators aiming at a deeper understanding of the chemiexcitation process in activated chemiluminescence. The results are analyzed in terms of adherence to the CIEEL mechanism and provide theoretical grounds for experimental observations. The chemiexcitation mechanisms of 1,2-dioxetane and 1,2-dioxetanone are comparatively discussed here for the first time, suggesting that the energetics of the intermolecular electron/charge transfer are related to the structure of the peroxide.

2 Computational details

MP2 calculations were performed using the Gaussian09 rev. D01 program package.[27] CASSCF/CASPT2 computations were carried out using the Molcas 8.0 suite of programs.[28]

2.1 Binding energies and vertical electron affinities

The ground-state geometries of isolated molecules and molecular complexes formed between cyclic peroxides and ACTs were optimized at the MP2/6-31++G(d,p) level.[29,30] Binding energies were calculated by subtracting the energies of the isolated molecules from the energy of their respective complexes. The basis set superposition error (BSSE) of the complexes was corrected using the counterpoise procedure.[31] Solvent effects were estimated using the polarizable continuum model with the integral equation formalism (IEFPCM) and using terms from the solvent model based on density (SMD) (hereafter, MP2-(SMD)/6-31++G(d,p) method).[32,33]

The energy needed for the peroxides to receive one electron at the neutral minimum geometry, *i.e.* their vertical electron affinity (VEA), has been computed at the same level of theory by subtracting the energy of the anionic species from the energy of the corresponding neutral species. On top of the MP2 geometries, the complete-active-space self-consistent field (CASSCF) method[34] was employed to build multiconfigurational neutral and anion wave functions, using the relativistic core correlation atomic natural orbital basis set (ANO-RCC) with valence triple-ζ plus polarization contraction (VTZP).[35] Details of the selected active spaces can be found in Sections 2.2 and 2.3. The complete-active-space second-order perturbation theory (CASPT2) method[36–38] was used to compute the dynamical electron correlation, in order to provide more accurate VEA values. An imaginary level shift of 0.2 a.u. was used to minimize the effect of weak intruder states,[39] whereas an ionization-potential electron-affinity (IPEA) shift of 0.25 a.u. was used to correct the underestimation of the energy of the anionic states relative to that of neutral states.[40,41]

2.2 Effect of peroxide bond elongation on transition energies

The effect of breaking the peroxide bond on the ground state energy of the molecular complex was investigated at the MP2/6-31++G(d,p) level. The O–O bond length was scanned from 153 to 198 pm in three steps of 15 pm and the resulting constrained structures were optimized. On top of the obtained geometries, the CASSCF method[34] and the ANO-RCC-VTZP basis set were used to explore the excited-state surfaces. The multiconfigurational wave functions of the 1,2-dioxetane–naphthalene system were built using two π and two π* orbitals from naphthalene, two n orbitals with π symmetry from the oxygen atoms and the σ and σ* orbitals from the O–O bond [(10,8) active space]. A better description of the 1,2-dioxetanone–naphthalene complex required the inclusion of the π and π* MOs of the C═O bond [(12,10) active space].

An overall number of sixty roots for the 1,2-dioxetane–naphthalene complex were required in the state average (SA) CASSCF procedure to track the high-energy charge-transfer state between the ACT and the peroxide. In contrast, only thirty roots were computed in each of the 1,2-dioxetanone–naphthalene complexes, as shall be discussed below. The dynamic electron correlation was quantified by means of the CASPT2 method, using the SA-CASSCF wave functions as a reference (SA-CASSCF/CASPT2 method). An imaginary shift of 0.2 a.u. and an IPEA shift of 0.00 a.u. were used for these calculations on neutral states.

2.3 Exploration of the CIEEL mechanism

Due to the lack of converged structures obtained at peroxide O–O distances larger than 198 pm using single-reference methods, the study of the chemiluminescence reaction profile in peroxide–ACT complexes beyond these points required the use of alternative computational strategies. Hence, the 1,2-dioxetanone coordinates of the 1,2-dioxetanone–anthracene complex obtained after optimization using the MP2 method were replaced by the accurate ground-state geometries previously reported for the unimolecular decomposition of 1,2-dioxetanone.[42] Thereby, the influence of the aromatic system on the peroxide electronic states was evaluated. The active space for the SA-CASSCF calculations comprised 14 electrons distributed into 12 MOs. The choice consisted, on the one hand, of the two n orbitals with π symmetry of the peroxide oxygen atoms and the σ and σ* orbitals of the O–O bond. On the other hand, the four π and four π* most relevant MOs of anthracene were also included in the active space. Since we were interested only in the low-lying states, four roots were required in the SA-CASSCF method. The smaller valence double-ζ plus polarization contraction of the ANO-RCC basis set (ANO-RCC-VDZP) was used throughout in order to make the computations affordable.[35] The dynamic electron correlation was computed using the CASPT2 method as explained above. An imaginary shift of 0.2 a.u. and an IPEA shift of 0.25 a.u. were used for these calculations on neutral states.

3 Results and discussion

3.1 Stability of molecular complexes of cyclic peroxides and ACTs

The equilibrium geometries of complexes formed by unsubstituted four-membered cyclic peroxides and naphthalene are depicted in Fig. 1. These model compounds were selected to keep the system small enough to allow accurate calculations.[42–46] Several initial configurations of each system were investigated and the lowest energy geometry of the computed π-bonded systems is in agreement with previously reported structures.[43] The class of the cyclic peroxide, *i.e.* 1,2-dioxetane or 1,2-dioxetanone, has a subtle effect

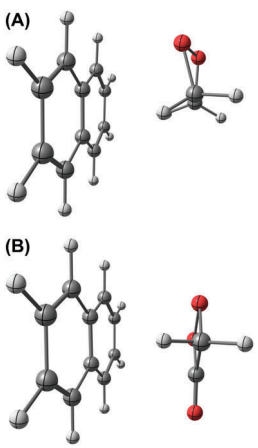

Fig. 1 MP2/6-31++G(d,p) optimized geometries of complexes between naphthalene and peroxides **1** (A) and **2** (B).

Table 1 Intermolecular distances (ID) and binding energies (BE) for the ACT–peroxide molecular complexes

Complex	ID[a] (pm)	BE (kJ mol^{-1})
Naphthalene-1,2-dioxetane	350	−18.1
Naphthalene-1,2-dioxetanone	320	−19.5
Naphthalene-tetramethyl-1,2-dioxetane	400	−16.0
Naphthalene-dimethyl-1,2-dioxetanone	350	−14.5
Anthracene-1,2-dioxetanone	320	−19.9
2-Napththolate-1,2-dioxetanone	310	−24.4

[a] Distance between the center of mass of the peroxide 4-membered ring and the center of mass of the aromatic rings interacting with it.

(<2.8 kJ mol^{-1}) on both binding energies (BE) and intermolecular distances (<50 pm) between the center of mass of the peroxide and the ACT (Table 1).

For non-methylated peroxides, binding energies increase with the inclusion of the carbonyl group probably due to the increase in both planarity and the number of π-bonds prone to π-stacking with the ACT (*i.e.* naphthalene). Even so, the difference in the obtained energies is too small to explain only by itself the difference in the efficiency of activated chemiluminescence observed experimentally.[16] As expected, methylated 1,2-dioxetanes and 1,2-dioxetanones have a lower binding energy with naphthalene compared to the corresponding parent compounds due to steric hindrance that compromises the parallel alignment between the peroxide and the ACT.[47] The effect of ACTs with decreasing oxidation potentials (naphthalene > anthracene > 2-naphththolate)[48] on the binding energy with 1,2-dioxetanone suggests that more oxidizable ACTs form more stable charge transfer (CT) molecular complexes.

3.2 Effect of peroxide bond elongation on transition energies

Complexes of peroxides **1** or **2** and naphthalene were used to compare the evolution of relevant states along the O–O bond opening coordinate (Fig. 2). For each complex, the transition energies were tracked using the CASPT2//MP2 methodology, elongating the initial optimized O–O bond distance of 153 pm in three steps of 15 pm. At O–O bond distances larger than 198 pm, the MP2 minimizations failed to converge due to the inaccurate description of the biradical wave function of the system by the single-reference method. However, a comparative trend of the transition energies can be disclosed with the converged structures. The states of interest are the ground state (closed shell that turns into a σ,σ* state as the O–O bond breaks), the intramolecular n,σ* state (unimolecular decomposition paths of **1** and **2**),[35,42] and the intermolecular π,σ* state (the CT state from the ACT to the peroxide).

Peroxide bond elongation increases the ground state energies of **1** and **2** (Fig. 2). Conversely, the energies of both n,σ* and π,σ* states decrease with O–O bond elongation. As the energy of the peroxide σ* orbital decreases, electron/charge transfer from the ACT to the cyclic peroxide becomes more thermodynamically feasible. The replacement of a C(sp^3)H$_2$ group by a C(sp^2)O group from 1,2-dioxetane to 1,2-dioxetanone markedly decreases the energy of the π,σ* state due to inductive effects and increase in planarity, whereas the energy of the n,σ* state is practically unaffected (Fig. 2).

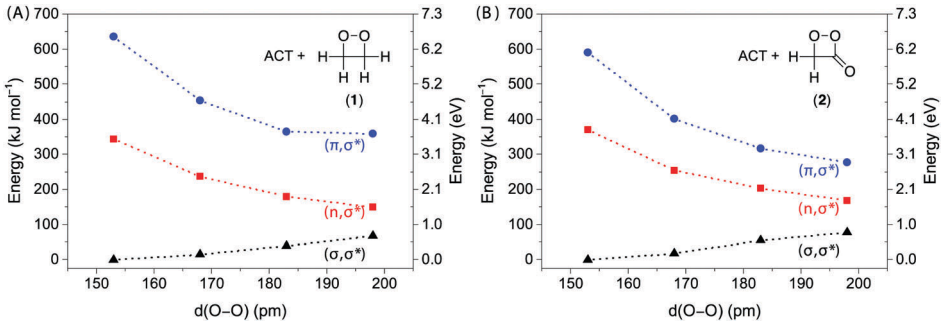

Fig. 2 Evolution of SA-CASSCF/CASPT2 energies of the three states of interest in the O–O bond breaking in molecular complexes formed by peroxides **1** and **2** with naphthalene.

The relative energies of the σ,σ*, n,σ* and π,σ* states for cyclic peroxides **1** and **2** clearly provide the theoretical grounds for the differential reactivity of 1,2-dioxetanes and 1,2-dioxetanones towards the ACT. The potential energy change for the elongation of the O–O bond of 1,2-dioxetane suggests that the electron/charge transfer from the ACT is less favorable than the unimolecular decomposition. Although the energy gap between the σ,σ* and π,σ* states of 1,2-dioxetanone is much lower (<200 kJ mol^{-1}) than that of 1,2-dioxetane (~ 350 kJ mol^{-1}), electron/charge transfer from the ACT is still less favorable than unimolecular decomposition, explaining the low efficiency of electron transfer catalysis involving 1,2-dioxetanones determined experimentally.[16,18]

3.3 Formation of radical anions of cyclic peroxides

Charge-transfer complexes are formed by the interaction of the HOMO of the ACT with the LUMO of the peroxide.[49] Accordingly, the stability constant of the CT complexes as well as the rate of electron/charge transfer should be related to the ionization potential of the ACT, the vertical electron affinity (VEA) of the peroxides and the binding energy between them.[50] Considering that the effect of the peroxide structure on the CT binding energy is small (Table 1), for a given ACT the VEA of the peroxide is expected to determine the complex stability.

VEA is related to the reduction potential and, therefore, the lower the VEA, the higher the amount of adiabatic energy for receiving an electron and reducing the peroxide. Radical ion formation after electron/charge transfer reduces the O–O bond order of 1,2-dioxetanes and 1,2-dioxetanones, facilitating the decomposition process.[44,45] The increase in the number of alkyl substituents decreases the VEA of cyclic peroxides, whereas the replacement of a C(sp^3)H$_2$ group by a C(sp^2)O group increases the VEA, as determined at the MP2 and CASPT2//MP2 levels (Table 2). Using toluene as solvent lessens the energy requirement for peroxide reduction without affecting this general trend. As the presence of methyl groups leads to a decrease in VEA values, electron transfer to the methyl-substituted peroxides is more difficult, whereas, the presence of a carbonyl group facilitates this transfer, making 1,2-dioxetanone more prone to activated decomposition as compared to 1,2-dioxetane (Table 2). These results confirm that the ratio between unimolecular decomposition and activated chemiluminescence is affected by the peroxide substitution pattern. In addition, it is expected to show a complex dependence on solvent properties, as already verified experimentally.[14,51–53]

Table 2 Vertical electron affinities (kJ mol^{-1}) of model peroxides

	MP2		
Peroxide	Gas phase[a]	Toluene[b]	CASPT2//MP2[c]
Tetramethyl-1,2-dioxetane	−175	−63	−142
1,2-Dioxetane (**1**)	−158	−35	−133
Dimethyl-1,2-dioxetanone	−88	26	−58
1,2-Dioxetanone (**2**)	−70	46	−42

[a] MP2/6-31++G(d,p) method. [b] MP2-(SMD)//MP2/6-31++G(d,p) methodology. [c] CASPT2//MP2/6-31++G(d,p) methodology.

3.4 Adherence to the CIEEL mechanism

We investigate the reasons for the inefficient activated chemiluminescence of 1,2-dioxetanones in terms of adherence to the CIEEL mechanism using the model molecular complex formed between the parent 1,2-dioxetanone (**2**) and anthracene. The diabatic representations of the ground state [^{1}(σ,σ*)], the most relevant excited states [^{3}(σ,σ*), ^{1,3}(n,σ*), and ^{1,3}(π,π*)], and the CT states [^{1,3}(π,σ*)] along the 1,2-dioxetanone decomposition reaction coordinate were calculated using peroxide geometries available in the literature (Fig. 3).[42] The potential energy curve corresponding to the unimolecular decomposition of **2** in the presence of the ACT [^{1}(σ,σ*)] agrees with previous reports on the isolated peroxide.[42,44,54–56] In the transition state region, intrinsic reaction coordinate (IRC) = 0.0 a.u., the ^{1}(σ,σ*) and ^{3}(σ,σ*) states have similar energies because during the unimolecular decomposition peroxide bond breaking leads to a vicinal biradical. Analogously, the ^{1}(n,σ*) and ^{3}(n,σ*) states are practically degenerate at the transition state as well as the CT ^{1}(π,π*) and ^{3}(π,π*) states (Fig. 3).

Complexation with the ACT increases the energy of the ^{1,3}(n,σ*) states of **2** and no evidence of conical intersection leading to the ground state biradical is observed (Fig. 3). Thus, the presence of anthracene does not significantly decrease the barrier for the thermal decomposition of 1,2-dioxetanone compared to the isolated peroxide. Accordingly, the experimental quantum yield and rate constant for the chemiluminescence of encumbered 1,2-dioxetanones do not depend on the ACT.[16,47] The ground state decomposition of **2** is the lowest energy reaction pathway even in the presence of the ACT; however,

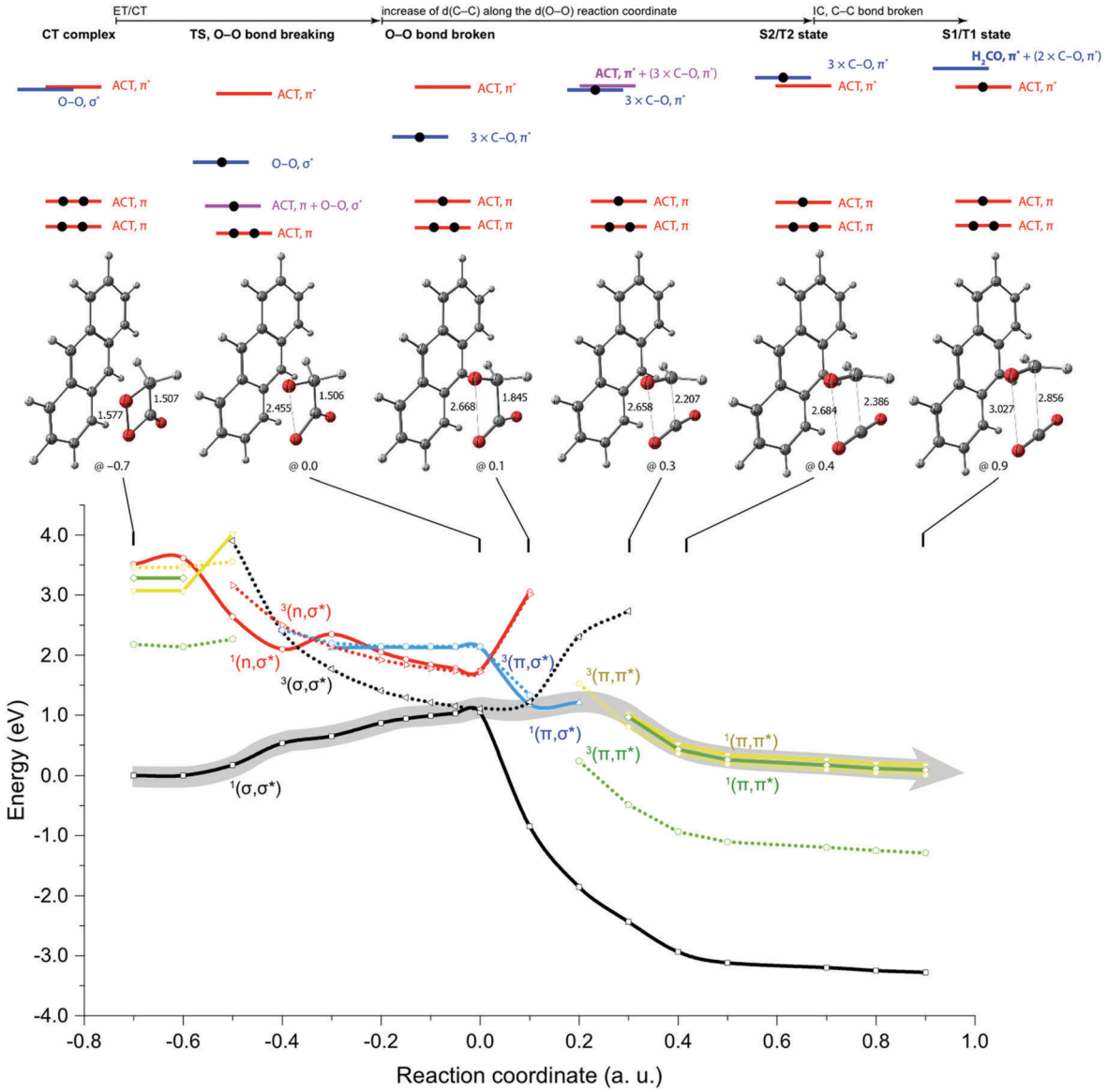

Fig. 3 SA-CASSCF/CASPT2 potential energy curves for the dissociation of a CT complex formed between 1,2-dioxetanone and anthracene. States $^{1,3}(\sigma,\sigma^*)$ and $^{1,3}(n,\sigma^*)$ are localized in 1,2-dioxetanone, whereas $^{1,3}(\pi,\pi^*)$ states are localized in the anthracene counterpart, and $^{1,3}(\pi,\sigma^*)$ states are of CT nature. Structures along selected reaction coordinates and the corresponding lengths of O–O and C–C bonds (d(O–O) and d(C–C), respectively) are depicted. The semi-quantitative orbital diagram shows the energies of the molecular orbitals of the ACT/1,2-dioxetanone supermolecule as determined at the CAM-B3LYP/aug-cc-pVDZ level. Electron occupancy was inferred to rationalize the experimental results. Orbital density at the ACT, peroxide/carbonyl compound, and both are marked in red, blue and magenta, respectively. The grey arrow indicates the singlet chemiexcitation pathway.

this fact alone cannot explain the extremely low efficiency of the activated decomposition of 1,2-dioxetanones.

At the transition state, the $^{1,3}(\pi,\sigma^*)$ CT states are 1.0 eV (96 kJ mol^{-1}) higher in energy than the $^{1,3}(\sigma,\sigma^*)$ states. However, the energy of the CT states decreases as the IRC moves forward and at IRC = 0.1 a.u. it matches with the energy of the $^3(\sigma,\sigma^*)$ state. In other words, as the O–O bond of the 1,2-dioxetanone–anthracene CT complex breaks, the ground state of the peroxide $^1(\sigma,\sigma^*)$ approaches the CT state $[^{1,3}(\pi,\sigma^*)]$ and departs from the direct population of excited states of carbonyl products $[^{1,3}(n,\sigma^*)]$. At the same time, the crossing between the $^1(\sigma,\sigma^*)$ and $^3(\sigma,\sigma^*)$ states allows, in principle, the population of both the $^{1,3}(\pi,\sigma^*)$ CT states. At IRC = 0.2, the crossing of $^{1,3}(\pi,\sigma^*)$ states with the $T_2[^3(\pi,\pi^*)]$, $T_1[^3(\pi,\pi^*)]$, $S_2[^1(\pi,\pi^*)]$ and $S_1[^1(\pi,\pi^*)]$ states is feasible.

These results suggest that ground state decomposition of 1,2-dioxetanone is the energetically favored reaction pathway in the presence of an ACT, thereby giving a reason for the low emission quantum yields observed experimentally[16,18] In addition, our calculations indicate that if excited states of the ACT were formed in this process, these should have triplet multiplicity and be non-emissive, due to their easy quenching.[57] The involvement of triplet-excited states of the ACT in the activated decomposition of 1,2-dioxetanone and similar compounds has

not yet been addressed experimentally, probably because it is difficult to design such an experiment since the addition of triplet energy acceptors can interfere in peroxide decomposition.

Our previous report on the activated decomposition of 1,2-dioxetanone proposed the formation of a supermolecule between the ACT and the peroxide interpreting the chemiexcitation process as an internal conversion.[47] The structures of **2** along the reaction coordinate were submitted to single point energy calculations, at the CAM-B3LYP/aug-cc-pVDZ level,[58,59] to obtain the molecular orbital energy diagram corresponding to the decomposition process. The results were analyzed in combination with the SA-CASSCF/CASPT2 data. The energy levels of the HOMO−1, HOMO, LUMO and LUMO+1 of the CT complex along the reaction coordinate are given in Fig. S1 (ESI†). The CT complex (IRC = −0.7 a.u.) is a closed shell system. Peroxide bond breaking favors the electron transfer from the ACT portion of the supermolecule to the 1,2-dioxetanone moiety, which has been observed experimentally for the activated decomposition of spiro-1,2-dioxetanones.[47,60] Therefore, at the TS, the O–O σ* orbital of the peroxide is now singly occupied. The nature of the initial HOMO has changed from a π orbital of the ACT to the combination of the ACT π orbital and the O–O σ* orbital.

After the O–O bond is broken (IRC = 0.1 a.u.), the C–C bond begins to break and, for the $^1(\pi,\sigma^*)$ electronic state, the singly occupied orbital is now formed by three C═O π* orbital contributions from the CO_2 and H_2CO moieties, together with the C–C σ orbital. As the C–C bond length increases (IRC = 0.3 a.u.), the energy of this singly occupied orbital increases accordingly and the orbital density from the three C═O π* orbitals mixes with the ACT π* orbital. At IRC = 0.4 a.u., the energy of the C═O π* orbital is higher than that of the ACT π* orbital. The states resulting from this electronic configuration are formally the S_2 or T_2 excited states and were formed during C–C bond breaking, in agreement with the diabatic surface calculated using the SA-CASSCF/CASPT2 method. However, at IRC = 0.4 a.u. the C–C bond is still not broken, as suggested by the bent geometry of both the CO_2 and H_2CO fragments. As the reaction coordinate moves forward, C–C bond breaking results in an excited ACT *via* internal conversion, as predicted in our previous report.[47] In the $^1(\pi,\pi^*)$ state, the LUMO+1 has a major contribution from the H_2CO π* orbital instead of being distributed towards three C═O π* orbitals of CO_2 and H_2CO moieties. In fact, orbital density increases at the H_2CO group and decreases at the CO_2 group as the C–C bond breaks. The reported orbital diagram cannot unequivocally distinguish singlet and triplet excited states, but it suggests that back electron transfer from $CO_2^{-\bullet}$ or $H_2CO^{-\bullet}$ to the ACT π* is not likely to occur; instead, after O–O bond breaking, chemiexcitation occurs concomitantly with C–C bond breaking. Our group has proposed before a similar chemiexcitation mechanism for the induced decomposition of phenoxyl-substituted 1,2-dioxetanes, where an intramolecular version of the CIEEL mechanism appears to operate.[52]

The calculated potential energy surfaces for the different electronic configurations and the energies of the relevant molecular orbitals of the supermolecule composed by the peroxide and the activator indicate that: (i) there is a crossing of the ground state surface $^1(\sigma,\sigma^*)$ with the lowest triplet state energy surface $^3(\sigma,\sigma^*)$ near the TS for O–O bond cleavage, (ii) the triplet state energy surface intersects with the $^{1,3}(\pi,\sigma^*)$ surfaces in a region where C–C bond cleavage is predominant, and (iii) the crossing of the $^{1,3}(\pi,\sigma^*)$ surface with the $^{1,3}(\pi,\pi^*)$ potential energy surface (PES) would enable the formation of the singlet and triplet-excited ACT. Triplet excited ACT molecules will not contribute to the CL emission since their excited state deactivation is non-radiative, occurring *via* inter-system crossing (ISC).[57] Additional validation of our theoretical findings requires an experimental approach able to provide unequivocal evidence of the involvement of triplet-excited ACT molecules in the decomposition of 1,2-dioxetanone. However, the detection of the triplet excited ACT in the catalyzed decomposition of 1,2-dioxetanones is difficult, if not impossible, because the unimolecular decomposition of these peroxides already produces triplet excited carbonyl compounds,[2,8,19] which can generate the triplet excited state of the ACT *via* energy transfer.

Briefly, the results pointed out above are compatible with the supermolecule model and suggest that either triplet or singlet excited states of the ACT can be formed in the activated decomposition of 1,2-dioxetanone. However, the excitation efficiency should be low, as the ground state PES constitutes the minimum energy pathway.

4 Conclusions

Unsubstituted 1,2-dioxetane and 1,2-dioxetanone form CT complexes with naphthalene, with the complex with 1,2-dioxetanone being slightly more stable, whereas methylated derivatives have lower binding energies in the complex. The energy gap between the ground state decomposition energy surface (σ,σ*) of 1,2-dioxetanone and the excited state surface in the presence of naphthalene (π,σ*) is significantly lower than for 1,2-dioxetanes, but still high. These facts explain preliminarily why 1,2-dioxetanes do not undergo ACT-catalyzed decomposition and 1,2-dioxetanones show low efficiency in this process. This approach will be utilized in the future also to rationalize the efficient excited state formation in the peroxyoxalate reaction, where the high-energy intermediate is supposed to be 1,2-dioxetanedione, which should interact more efficiently with the ACT.[47] The results of CASSCF/CASPT2 calculations of the PES and the calculated molecular orbital energies of the supermolecule anthracene–1,2-dioxetanone show that the ground state energy surface is the lowest energy PES, explaining the observed low efficiency of the chemiexcitation process. This low efficiency might also be caused by late C–C bond breaking, which favors the thermal unimolecular pathway. These assumptions are compatible with the supermolecule model, where chemiexcitation is described as a sequence of electron transfer and internal conversion. Formal electron or charge back transfers are not involved, since the ACT and the carbonyl products form a supermolecule, which is sensitive to medium and structural effects. Accordingly, the solvent and the structure of the peroxide modulate the relative energy of the (n,σ*) and (π,π*) states and, therefore, activated

chemiluminescence could be possible (and even efficient) depending on the system and reaction conditions. This theory will be tested in the future with 1,2-dioxetanedione as the peroxide and the approach utilized here. Finally, our results suggest that chemiexcitation could *a priori* produce the ACT molecules in either singlet or triplet electronically excited states. The triplet chemiexcitation of the ACT should be tested experimentally, although this might not be a simple task.

Acknowledgements

F. A. A. thanks Capes (Coordenação de Aperfeiçoamento de Pessoal de Nível Superior) for a PhD fellowship (PROEX) and for a PDSE internship (0285/2014-5). E. L. B. (grant 2014/14866-2) and W. J. B. (grant 2014/22136-4) thank FAPESP (São Paulo Research Foundation) for financial support. A. F. M. and D. R. S. are grateful to Ministerio de Economía y Competitividad (project CTQ2014-58624-P, ''Juan de la Cierva'' grant JCI-2012-13431, FPI grant BES-2011-048326, and the mobility program EEBB-I-14-08821). R. L. acknowledges the Swedish Research Council (Grant No. 2012-3910) and eSSENCE for financial support.

References

1 L. F. M. L. Ciscato, F. A. Augusto, D. Weiss, F. H. Bartoloni, S. Albrecht, H. Brandl, T. Zimmermann and W. J. Baader, *ARKIVOC*, 2012, 391–430.
2 W. J. Baader, C. V. Stevani and E. L. Bastos, Chemiluminescence of Organic Peroxides, in *The Chemistry of Peroxides*, ed. Z. Rappoport, John Wiley & Sons, Ltd, Chichester, 2006, pp. 1211–1278.
3 W. Adam, D. Reinhardt and C. R. Saha-Möller, *Analyst*, 1996, **121**, 1527–1531.
4 A. Roda, M. Mirasoli, E. Michelini, M. Di Fusco, M. Zangheri, L. Cevenini, B. Roda and P. Simoni, *Biosens. Bioelectron.*, 2016, **76**, 164–179.
5 W. Adam and W. J. Baader, *Angew. Chem., Int. Ed.*, 1984, **23**, 166–167.
6 W. Adam and W. J. Baader, *J. Am. Chem. Soc.*, 1985, **107**, 410–416.
7 E. L. Bastos and W. J. Baader, *ARKIVOC*, 2007, 257–272.
8 N. J. Turro, P. Lechtken, G. Schuster, J. Orell and H. Steinmet, *J. Am. Chem. Soc.*, 1974, **96**, 1627–1629.
9 S. P. Schmidt and G. B. Schuster, *J. Am. Chem. Soc.*, 1978, **100**, 5559–5561.
10 G. B. Schuster, *Acc. Chem. Res.*, 1979, **12**, 366–373.
11 J. Y. Koo, S. P. Schmidt and G. B. Schuster, *Proc. Natl. Acad. Sci. U. S. A.*, 1978, **75**, 30–33.
12 L. F. M. L. Ciscato, F. H. Bartoloni, E. L. Bastos and W. J. Baader, *J. Org. Chem.*, 2009, **74**, 8974–8979.
13 C. V. Stevani, S. M. Silva and W. J. Baader, *Eur. J. Org. Chem.*, 2000, 4037–4046.
14 W. Adam, I. Bronstein, A. V. Trofimov and R. F. Vasil'ev, *J. Am. Chem. Soc.*, 1999, **121**, 958–961.
15 W. Adam, I. Bronstein, B. Edwards, T. Engel, D. Reinhardt, F. W. Schneider, A. V. Trofimov and R. F. Vasil'ev, *J. Am. Chem. Soc.*, 1996, **118**, 10400–10407.
16 M. A. de Oliveira, F. H. Bartoloni, F. A. Augusto, L. F. M. L. Ciscato, E. L. Bastos and W. J. Baader, *J. Org. Chem.*, 2012, **77**, 10537–10544.
17 F. A. Augusto, G. A. de Souza, S. P. de Souza, M. Khalid and W. J. Baader, *Photochem. Photobiol.*, 2013, **89**, 1299–1317.
18 L. H. Catalani and T. Wilson, *J. Am. Chem. Soc.*, 1989, **111**, 2633–2639.
19 T. Wilson, Mechanisms of peroxide chemiluminescence, in *Singlet Oxygen*, ed. A. Frimer, CRC, Boca Raton, 1985, vol. 2, pp. 37–65.
20 H. Isobe, Y. Takano, M. Okumura, S. Kuramitsu and K. Yamaguchi, *J. Am. Chem. Soc.*, 2005, **127**, 8667–8679.
21 H. Isobe, S. Yamanaka, M. Okumura and K. Yamaguchi, *Luminescence*, 2008, **23**, 74.
22 K. Yamaguchi, H. Isobe, S. Yamanaka and M. Okumura, Charge-transfer-induced luminescence (CTIL) mechanisms of chemi- and bioluminescence reactions, in *Bioluminescence and Chemiluminescence. Light Emission, Biology and Scientific Applications*, ed. X. Shen, X.-L. Yang, X.-R. Zhang, Z. J. Cui, L. J. Kricka and P. E. Stanley, World Scientific Publishing Co. Pte. Ltd., Singapore, 2009, pp. 261–264.
23 J. K. Kochi, *Angew. Chem., Int. Ed.*, 1988, **27**, 1227–1266.
24 L. F. M. L. Ciscato, F. H. Bartoloni, D. Weiss, R. Beckert and W. J. Baader, *J. Org. Chem.*, 2010, **75**, 6574–6580.
25 C. Hou, Y. J. Liu, N. Ferré and W. H. Fang, *Chem. – Eur. J.*, 2014, **20**, 7979–7986.
26 Y. Takano, T. Tsunesada, H. Isobe, Y. Yoshioka, K. Yamaguchi and I. Saito, *Bull. Chem. Soc. Jpn.*, 1999, **72**, 213–225.
27 M. J. Frisch, G. W. Trucks, H. B. Schlegel, G. E. Scuseria, M. A. Robb, J. R. Cheeseman, G. Scalmani, V. Barone, B. Mennucci, G. A. Petersson, H. Nakatsuji, M. Caricato, X. Li, H. P. Hratchian, A. F. Izmaylov, J. Bloino, G. Zheng, J. L. Sonnenberg, M. Hada, M. Ehara, K. Toyota, R. Fukuda, J. Hasegawa, M. Ishida, T. Nakajima, Y. Honda, O. Kitao, H. Nakai, T. Vreven, J. A. Montgomery Jr., J. E. Peralta, F. Ogliaro, M. J. Bearpark, J. Heyd, E. N. Brothers, K. N. Kudin, V. N. Staroverov, R. Kobayashi, J. Normand, K. Raghavachari, A. P. Rendell, J. C. Burant, S. S. Iyengar, J. Tomasi, M. Cossi, N. Rega, N. J. Millam, M. Klene, J. E. Knox, J. B. Cross, V. Bakken, C. Adamo, J. Jaramillo, R. Gomperts, R. E. Stratmann, O. Yazyev, A. J. Austin, R. Cammi, C. Pomelli, J. W. Ochterski, R. L. Martin, K. Morokuma, V. G. Zakrzewski, G. A. Voth, P. Salvador, J. J. Dannenberg, S. Dapprich, A. D. Daniels, Ö. Farkas, J. B. Foresman, J. V. Ortiz, J. Cioslowski and D. J. Fox, *Gaussian09 v. D.01*, 2009.
28 F. Aquilante, J. Autschbach, R. K. Carlson, L. F. Chibotaru, M. G. Delcey, L. De Vico, I. Fdez. Galván, N. Ferré, L. M. Frutos, L. Gagliardi, M. Garavelli, A. Giussani, C. E. Hoyer, G. Li Manni, H. Lischka, D. X. Ma, P. Å. Malmqvist, T. Muller, A. Nenov, M. Olivucci, T. B. Pedersen, D. L. Peng, F. Plasser, B. Pritchard, M. Reiher, I. Rivalta, I. Schapiro, J. Segarra-Martí, M. Stenrup, D. G. Truhlar,

L. Ungur, A. Valentini, S. Vancoillie, V. Veryazov, V. P. Vysotskiy, O. Weingart, F. Zapata and R. Lindh, *J. Comput. Chem.*, 2016, **37**, 506–541.
29 M. Head-Gordon, J. A. Pople and M. J. Frisch, *Chem. Phys. Lett.*, 1988, **153**, 503–506.
30 M. J. Frisch, J. A. Pople and J. S. Binkley, *J. Chem. Phys.*, 1984, **80**, 3265–3269.
31 S. F. Boys and F. Bernardi, *Mol. Phys.*, 1970, **19**, 553–566.
32 A. V. Marenich, C. J. Cramer and D. G. Truhlar, *J. Phys. Chem. B*, 2009, **113**, 6378–6396.
33 J. Tomasi, B. Mennucci and R. Cammi, *Chem. Rev.*, 2005, **105**, 2999–3093.
34 B. O. Roos, P. R. Taylor and P. E. M. Siegbahn, *Chem. Phys.*, 1980, **48**, 157–173.
35 B. O. Roos, R. Lindh, P. Å. Malmqvist, V. Veryazov and P. O. Widmark, *J. Phys. Chem. A*, 2004, **108**, 2851–2858.
36 K. Andersson, P. Å. Malmqvist, B. O. Roos, A. J. Sadlej and K. Wolinski, *J. Phys. Chem.*, 1990, **94**, 5483–5488.
37 K. Andersson, P. Å. Malmqvist and B. O. Roos, *J. Chem. Phys.*, 1992, **96**, 1218–1226.
38 D. Roca-Sanjuán, F. Aquilante and R. Lindh, *Wiley Interdiscip. Rev.: Comput. Mol. Sci.*, 2012, **2**, 585–603.
39 N. Forsberg and P. A. Malmqvist, *Chem. Phys. Lett.*, 1997, **274**, 196–204.
40 D. Roca-Sanjuán, M. Merchán, L. Serrano-Andrés and M. Rubio, *J. Chem. Phys.*, 2008, **129**, 095104.
41 A. Francés-Monerris, J. Segarra-Martí, M. Merchán and D. Roca-Sanjuán, *J. Chem. Phys.*, 2015, **143**, 215101.
42 F. Y. Liu, Y. J. Liu, L. De Vico and R. Lindh, *J. Am. Chem. Soc.*, 2009, **131**, 6181–6188.
43 A. J. A. Aquino, I. Borges, R. Nieman, A. Kohn and H. Lischka, *Phys. Chem. Chem. Phys.*, 2014, **16**, 20586–20597.
44 L. De Vico, Y. J. Liu, J. W. Krogh and R. Lindh, *J. Phys. Chem. A*, 2007, **111**, 8013–8019.
45 F. Y. Liu, Y. J. Liu, L. De Vico and R. Lindh, *Chem. Phys. Lett.*, 2009, **484**, 69–75.
46 P. Farahani, M. Lundberg, R. Lindh and D. Roca-Sanjuán, *Phys. Chem. Chem. Phys.*, 2015, **17**, 18653–18664.
47 F. H. Bartoloni, M. A. de Oliveira, L. F. M. L. Ciscato, F. A. Augusto, E. L. Bastos and W. J. Baader, *J. Org. Chem.*, 2015, **80**, 3745–3751.
48 G. J. Hoijtink, *Recl. Trav. Chim. Pays-Bas*, 1958, **77**, 555–558.
49 I. Shokaryev, A. J. C. Buurma, O. D. Jurchescu, M. A. Uijttewaal, G. A. de Wijs, T. T. M. Palstra and R. A. de Groot, *J. Phys. Chem. A*, 2008, **112**, 2497–2502.
50 K. P. Goetz, D. Vermeulen, M. E. Payne, C. Kloc, L. E. McNeil and O. D. Jurchescu, *J. Mater. Chem. C*, 2014, **2**, 3065–3076.
51 W. Adam, I. Bronstein and A. V. Trofimov, *J. Phys. Chem. A*, 1998, **102**, 5406–5414.
52 E. L. Bastos, S. M. da Silva and W. J. Baader, *J. Org. Chem.*, 2013, **78**, 4432–4439.
53 M. Khalid, S. P. Souza, L. F. M. L. Ciscato, F. H. Bartoloni and W. J. Baader, *Photochem. Photobiol. Sci.*, 2015, **14**, 1296–1305.
54 L. Yue, D. Roca-Sanjuán, R. Lindh, N. Ferré and Y. J. Liu, *J. Chem. Theory Comput.*, 2012, **8**, 4359–4363.
55 L. P. da Silva and J. C. G. E. da Silva, *ChemPhysChem*, 2013, **14**, 1071–1079.
56 L. P. da Silva and J. C. G. E. da Silva, *Struct. Chem.*, 2014, **25**, 1075–1081.
57 N. J. Turro, V. Ramamurthy and J. C. Scaiano, *Modern molecular photochemistry of organic molecules*, University Science Books, Sausalito, 2010.
58 T. H. Dunning, *J. Chem. Phys.*, 1989, **90**, 1007–1023.
59 T. Yanai, D. P. Tew and N. C. Handy, *Chem. Phys. Lett.*, 2004, **393**, 51–57.
60 F. H. Bartoloni, M. A. de Oliveira, L. F. M. L. Ciscato, F. A. Augusto, E. L. Bastos and W. J. Baader, *Luminescence*, 2014, **29**, 10.

